JOURNAL OF GEOPHYSICAL RESEARCH, VOL. 95, NO. C2, PAGES 1523–1536, FEBRUARY 15, 1990

An Analytical Study of the Frictional Response of Coastal Currents and Upwelling to Wind Stress

GIANNI A. DALU[1]

Cooperative Institute for Research in the Atmosphere, Fort Collins, Colorado

ROGER A. PIELKE

Department of Atmospheric Science, Colorado State University, Fort Collins

In this paper we present several theoretical results concerning currents forced by the wind in coastal regions, for a shallow sea and for a very deep sea. We investigate the time behavior and the spatial structure of the stream function and the momentum components, i.e., the onset, the transient, the asymptotic, and the periodic behavior of the currents and of the upwelling, forced by winds of different spatial and time structures. Results show that the intensity of the along coast jet initially grows linearly under a δ in time wind impulse, quadratically under a Heaviside in time wind impulse, and cubically under a linearly growing wind impulse. The asymptotic state is such that the intensity of the current vanishes if the wind impulse has a finite duration, while the intensity of the sea current has a final finite amplitude if the wind intensity goes to some finite value. If the wind stress is periodic in time, there is upwelling only when the period of the forcing is longer than a characteristic time scale, which is the sum of the inertial period and the friction e-folding time. Otherwise there are waves which propagate away from the region where the wind stress is acting. The spatial structure is such that the upwelling occurs in a horizontal region of the order of the Rossby deformation radius, corrected by the effect of friction (and by the effect of periodicity, when the wind stress is periodic in time). However, the horizontal gradient of the wind stress can be more important than the Rossby deformation radius in determining the horizontal extent of the upwelling region.

INTRODUCTION

Winds play an important role in coastal water currents and in the generation of upwelling [*Mizzi and Pielke*, 1984; *Dalu et al.*, 1989]. This upwelling is essential in order to maintain the fish-rich coastal waters. Furthermore, the coastal currents and the vertical mixing within the diurnal thermocline [*Dalu and Purini*, 1980, 1981] are very effective in dispersing pollutants in coastal waters close to large ports or heavily industrialized and urbanized areas.

There are numerous papers concerning upwelling and coastal currents induced by wind stress. Here we present a linear theory for the upwelling on an f plane in a continuously stratified sea. We choose to approach the problem analytically because some features, such as the upwelling and the coastal jet, are relatively poorly resolved by numerical models [*Clancy et al.*, 1979; *Huss and Feliks*, 1981]. Some authors deal with the onset of upwelling as a response to an impulsively applied wind stress [*Crepon et al.*, 1984; *Allen*, 1973]. Others are concerned about the stochastic aspect of the upwelling [*Carton and Philander*, 1984] or about their steady state features [*Middleton and Thompson*, 1985]. We revisit some of these results in rather general terms. Furthermore we add the case of periodic wind forcing, which leads to some interesting results, such as the possible presence of propagating waves at low latitude.

We present the solutions in terms of Green function theory for the spatial structure and in terms of Laplace transform theory for the time evolution. This presentation allows an overall view of the behavior of the coastal sea currents, which is more difficult to see when the solution is written as a sum of eigenfunctions of the system [*Kundu*, 1984].

For a description of the phenomenology associated with wind-driven coastal currents, see the paper by *Winant* [1980] and the proceedings of the coastal upwelling conference edited by *Richards* [1981].

2. EQUATIONS AND BOUNDARY CONDITIONS

The two-dimensional linearized equations, describing the coastal water flow induced by the wind stress, are

$$\left(\frac{\partial}{\partial t}+\lambda\right)u - fv + \frac{\partial}{\partial x}\Phi = \frac{\partial}{\partial z}\Upsilon^x \tag{1}$$

$$\left(\frac{\partial}{\partial t}+\lambda\right)v + fu = \frac{\partial}{\partial z}\Upsilon^y \tag{2}$$

$$\left(\frac{\partial}{\partial t}+\lambda\right)w - b + \frac{\partial}{\partial z}\Phi = 0 \tag{3}$$

$$\left(\frac{\partial}{\partial t}+\lambda\right)b + N^2 w = \frac{\partial}{\partial z}Q \tag{4}$$

$$\frac{\partial}{\partial x}u + \frac{\partial}{\partial z}w = 0 \tag{5}$$

where f is the Coriolis parameter, b is the buoyancy force, N is the Brunt-Väisälä frequency, Φ is the pressure term, and λ^{-1} is the damping time; i.e., the e folding time of the amplitude of the corresponding variable (the persistency of

[1]Also at Institute for Atmospheric Physics, Rome.

Paper number 89JC01376.
0148-0227/90/89JC-01376$05.00

the perturbation). The dissipation in coastal areas of the ocean is due to bottom friction [*Mofjeld*, 1988; *Dewey and Crawford*, 1988], to side-wall friction [*Pedlosky*, 1979], and to internal shear. The Rayleigh friction λ is a parameterization of the sum of these dissipative losses. The coastal waters are forced mechanically by the wind stress Υ, and thermally by the diabatic source of buoyancy Q. Υ and Q are assumed linearly decreasing from the sea surface to a depth h, where they vanish; i.e., their vertical gradient is constant through the layer $-h \le z \le 0$, and zero for $z < -h$.

Defining the stream function

$$u = \frac{\partial}{\partial z}\psi \qquad w = -\frac{\partial}{\partial x}\psi \tag{6}$$

the primitive equations (1)–(5), using (6), can be reduced to a single equation for the stream function:

$$\left[\left(\frac{\partial}{\partial t}+\lambda\right)^2 + N^2\right]\frac{\partial^2}{\partial x^2}\psi + \left[\left(\frac{\partial}{\partial t}+\lambda\right)^2 + f^2\right]\frac{\partial^2}{\partial z^2}\psi = \left(\frac{\partial}{\partial t}+\lambda\right)\frac{\partial^2}{\partial z^2}\Upsilon^x + f\frac{\partial^2}{\partial z^2}\Upsilon^y - \frac{\partial^2}{\partial z\,\partial x}Q \tag{7}$$

In Appendix A we define the nondimensional quantities and their Laplace transform. We denote with the circumflex the Laplace transformed variable, and with the tilde the corresponding nondimensional variable. Using the definition stated in Appendix A for the nondimensional variables and for their Laplace transform, the stream function equation (7) can be written as

$$\frac{\partial^2}{\partial \xi^2}\hat{\psi} + \frac{\partial^2}{\partial \eta^2}\hat{\psi} = \beta(p)\left[p\frac{\partial^2}{\partial \eta^2}\hat{\Upsilon}^\xi + \tilde{f}\frac{\partial^2}{\partial \eta^2}\hat{\Upsilon}^\zeta\right] - \beta'(p)\frac{\partial^2}{\partial \eta\,\partial \xi}\hat{Q} \tag{8}$$

2.1. *The Boundary Conditions*

The boundary conditions for a sea of finite depth H are

$$\hat{\psi}(\xi = 0, \eta) = 0 \qquad \hat{\psi}(\xi = \infty, \eta) = 0$$
$$\hat{\psi}(\xi, \eta = 0) = 0 \qquad \hat{\psi}(\xi, \eta = -\tilde{H}) = 0 \tag{9}$$

where $\tilde{H} = H/h$ is the sea depth normalized to the depth of the mixed layer h.

The boundary conditions for an infinitely deep sea ($H \gg h$) are

$$\hat{\psi}(\xi = 0, \eta) = 0 \qquad \hat{\psi}(\xi = \infty, \eta) = 0$$
$$\hat{\psi}(\xi, \eta = 0) = 0 \qquad \hat{\psi}(\xi, \eta = -\infty) = 0 \tag{10}$$

2.2. *The Green Functions*

The Green function g which satisfies (8) with the boundary conditions (9) (sea of finite depth) is

$$g_\psi = -\frac{1}{2\pi}\ln\left[\frac{\cosh(\pi/\tilde{H})\xi_{0-} - \cos(\pi/\tilde{H})\eta_{0+}}{\cosh(\pi/\tilde{H})\xi_{0-} - \cos(\pi/\tilde{H})\eta_{0-}}\,\frac{\cosh(\pi/\tilde{H})\xi_{0+} - \cos(\pi/\tilde{H})\eta_{0-}}{\cosh(\pi/\tilde{H})\xi_{0+} - \cos(\pi/\tilde{H})\eta_{0+}}\right]^{1/2} \tag{11}$$

while the Green function g which satisfies (8) with the boundary conditions (10) (sea of infinite depth) is

$$g_\psi = -\frac{1}{2\pi}\ln\left[\frac{\xi_{0-}^2 + \eta_{0+}^2}{\xi_{0-}^2 + \eta_{0-}^2}\,\frac{\xi_{0+}^2 + \eta_{0-}^2}{\xi_{0+}^2 + \eta_{0+}^2}\right]^{1/2} \tag{12}$$

$$\xi_{0+} = (\xi + \xi') \qquad \xi_{0-} = (\xi - \xi')$$
$$\eta_{0+} = (\eta + \eta') \qquad \eta_{0-} = (\eta - \eta')$$

The Green functions for the velocities are given in Appendix B.

3. The Wind Stress and Thermal Forcing

The coastal waters are forced by the wind stress Υ:

$$\Upsilon^x(x, z) = \Upsilon_0 F(x, z, t)\sin\alpha$$
$$\Upsilon^y(x, z) = \Upsilon_0 F(x, z, t)\cos\alpha \tag{13}$$
$$\alpha = \tan^{-1}\frac{u_a}{v_a} \qquad \Upsilon_0 = \frac{\rho_a}{\rho_w}C_D u_a^2$$

and by the diabatic source of buoyancy Q:

$$Q = Q_0 F(x, z, t) \qquad Q_0 = g\alpha_T\frac{H_s - L_T E_v}{c_{p_w}\rho_w} \tag{14}$$

In (13) and (14) $F(x, z, t)$ is a function which describes the time behavior and the spatial distribution of the stress and the diabatic flux within the marine thermocline. The value of $\alpha_T = -1 \times 10^{-3}$ K is the thermal expansion coefficient of the water [*Defant*, 1961]. H_s is the sensible heat flux, E_v is the evaporation rate, and q and θ are the specific humidity and the potential temperature of the air [*Roll*, 1965]:

$$H_s = c_{p_a}\rho_a C_D u_a(\theta_a - \theta_w) \qquad E_v = C_D u_a(q_a - q_w)$$

When $u_a = 10$ m/s and $C_D = 2.5 \times 10^{-3}$ [*Geernaert*, 1988], we have

$$\Upsilon_0 = \frac{\rho_a}{\rho_w}C_D u_a^2 \approx 2.5 \times 10^{-4}\ \mathrm{m^2/s^2} \tag{15}$$

When $H_s - L_T E_v = 100$ W/m^2, we have

$$Q_0 = g\alpha_T\frac{H_s - L_T E_v}{c_{p_w}\rho_w} \approx 2.5 \times 10^{-8}\ \mathrm{m^2/s^3} \tag{16}$$

From (7)–(8), for the values given in (15)–(16), we see that the diabatic contribution is negligible when

$$Q_0\frac{\tilde{}}{hl} \ll \Upsilon_0\frac{[\lambda\sin\alpha + f\cos\alpha]}{h^2} \tag{17a}$$

i.e., when

$$l \gg h \tag{17b}$$

where l is the horizontal scale of the forcing. Since the horizontal scale l is usually much larger than the vertical scale h, the inequality (17) is usually fulfilled. Therefore we will drop the diabatic term in (7)–(8).

From *Mofjeld* [1988] and *Dewey and Crawford* [1988], we deduce an e-folding time of the order of 1 day:

$$\lambda^{-1} = O(1 \text{ day}) \tag{18}$$

In regions where the ocean is deep, λ can be smaller, and the e-folding time can be of the order of several days.

Assuming $h \approx 50$ m, the order of magnitudes of the intensity of the sea current and of the upwelling are

$$\overline{u_0} = u_0[\tilde{\lambda} \sin \alpha + \tilde{f} \cos \alpha] \approx 10 \text{ cm/s} \qquad u_0 = \Upsilon_0 \frac{T}{h}$$
$$\overline{w_0} = w_0[\tilde{\lambda} \sin \alpha + \tilde{f} \cos \alpha] \approx \text{mm/s} \qquad w_0 = u_0 \frac{h}{R} \tag{19}$$

respectively. R is the horizontal scale of the overturning, i.e., the horizontal scale of the upwelling, and T is the characteristic response time of the system. The intensity of the upwelling is proportional to the alongshore wind stress through inertia and proportional to the offshore wind stress through friction.

The sea temperature perturbation, ST, is proportional to the sum of the diabatic source and the vertical velocity, integrated in time. The order of magnitude of the intensity of ST is

$$\overline{b_0} = \frac{Q_0}{h\lambda} - \frac{N^2\overline{w_0}}{\lambda} \approx -\frac{N^2\overline{w_0}}{\lambda}$$
$$\text{ST} = -\overline{b_0}\frac{1}{g\alpha_T} = \frac{N^2\overline{w_0}}{\lambda}\frac{1}{g\alpha_T} \approx 0.1 \text{ K} \tag{20}$$

i.e., the thermal feedback from the sea to the atmosphere is negligible where the local winds have a diurnal variability (e.g., the sea breezes, as confirmed by numerical modeling studies by *Mizzi and Pielke* [1984] and by *Clancy et al.* [1979]). When the wind stress is persistent ($t \gg T$) and the dissipation λ is small, such as in the major regions of upwelling, the diabatic term may play an important role, and a large sea surface temperature anomaly can build up, because of the combined contributions of the diabatic source and the upwelling.

We write the normalized wind stress as a product of three functions of horizontal coordinate, of the vertical coordinate, and of time:

$$\tilde{F}(\xi, \eta, \tau) = \tilde{F}_1(\xi)\tilde{F}_2(\eta)\tilde{F}_3(\tau) \tag{21}$$

respectively. For the horizontal structure of the wind stress, we discuss the following cases:

Infinite fetch with constant wind stress

$$\tilde{F}_1(\xi) = He(\xi) \qquad 0 < \xi < \infty \tag{22}$$

Finite fetch with constant wind stress

$$\tilde{F}_1(\xi) = He(\xi) - He(\xi - \tilde{l}) \qquad 0 < \xi < \infty \tag{23}$$

Finite fetch with increasing and decreasing wind stress

$$\tilde{F}_1(\xi) = [He(\xi) - He(\xi - \tilde{l})]\frac{\xi}{\tilde{l}} + [He(\xi - \tilde{l}) - He(\xi - 2\tilde{l})]\frac{2\tilde{l} - \xi}{\tilde{l}} \tag{24}$$

Finite fetch with decreasing and increasing wind stress

$$\tilde{F}_1(\xi) = [He(\xi) - He(\xi - \tilde{l})]\frac{\tilde{l} - \xi}{\tilde{l}} + [He(\xi - \tilde{l}) - He(\xi - 2\tilde{l})]\frac{\xi - \tilde{l}}{\tilde{l}}$$

We assume that the wind stress is linearly distributed through the thermocline:

$$\tilde{F}_2(\eta) = \eta + 1 \qquad -1 < \eta < 0$$
$$\tilde{F}_2(\eta) = 0 \qquad \eta < -1$$

For the time structure, we discuss the following cases:

Dirac δ function impulse

$$\tilde{F}_3(\tau) = \delta(\tau) \Rightarrow \hat{F}_3(s) = 1$$

Impulse of infinite duration

$$\tilde{F}_3(\tau) = He(\tau) \Rightarrow \hat{F}_3(s) = \frac{1}{s}$$

Impulse of finite duration

$$\tilde{F}_e(\tau) = He(\tau) - He(\tau - \tilde{a}) \Rightarrow \hat{F}_3(s) = \frac{1}{s}[1 - \exp(-\tilde{a}s)]$$

Linearly growing impulse

$$\tilde{F}_3(\tau) = \tilde{a}\tau \Rightarrow \hat{F}_3(s) = \frac{\tilde{a}}{s^2}$$

Finally, we will discuss in some length the sea current induced by the sea breeze (equation (13)):

$$\sin \alpha = \sin \tilde{\omega}\tau \qquad \cos \alpha = \cos \tilde{\omega}\tau \tag{31}$$

4. Response to a Wind Stress of General Time Dependence

The governing equation for the stream function ψ, for the forcing specified in (21), is

$$\frac{\partial^2}{\partial \xi^2}\hat{\psi} + \frac{\partial^2}{\partial \eta^2}\hat{\psi} = \beta(p)\hat{\Upsilon}_0\hat{F}_3(s)\left\{[p \sin \alpha + \tilde{f} \cos \alpha]\hat{F}_1(\xi)\frac{\partial^2}{\partial \eta^2}\hat{F}_2(\eta)\right\} \tag{32}$$

4.1. *Transfer Functions: Response to a δ in Time Forcing*

Having derived the Green functions g in Appendix B, we can compute the transfer functions $\hat{G}$, i.e., the response of the sea current, as a physical system, to a $\delta(\tau)$ forcing:

$$\tilde{F}_3 = \delta(\tau) \Rightarrow \hat{F}_3 = 1 \tag{33}$$

For the wind stress, the transfer functions $\hat{G}_\Upsilon$ are

$$\hat{G}_{\psi Y}(\xi, \eta, s) = \beta(p)[p \sin \alpha + \tilde{f} \cos \alpha] \cdot \left\langle g_{\psi}, \hat{F}_1(\xi) \frac{\partial^2}{\partial \eta^2} \hat{F}_2(\eta) \right\rangle_{\xi', \eta'} \quad (34a)$$

$$\hat{G}_{uY}(\xi, \eta, s) = \beta(p)[p \sin \alpha + \tilde{f} \cos \alpha] \cdot \left\langle g_{u}, \hat{F}_1(\xi) \frac{\partial^2}{\partial \eta^2} \hat{F}_2(\eta) \right\rangle_{\xi', \eta'} \quad (34b)$$

$$\hat{G}_{wY}(\xi, \eta, s) = \beta(p)[p \sin \alpha + \tilde{f} \cos \alpha] \cdot \left\langle g_{w}, \hat{F}_1(\xi) \frac{\partial^2}{\partial \eta^2} \hat{F}_2(\eta) \right\rangle_{\xi', \eta'} \quad (34c)$$

where

$$\langle g, \hat{F} \rangle_{\xi', \eta'} = \int_0^{\infty} d\xi' \int_{-\hat{H}}^{0} d\eta' g(\xi - \xi', \eta - \eta') \hat{F}(\xi', \eta') \quad (35)$$

4.2. *Response to a Forcing of General Time Dependence*

For a general time behavior of the forcing,

$$\tilde{F}_3(\tau) \Rightarrow \hat{F}_3(s) \quad (36)$$

the response of the sea current is

$$\hat{\psi} = \hat{G}_{\psi Y} \tilde{Y}_0 \hat{F}_3(s) = \hat{F}_3(s) \beta(p) \tilde{Y}_0 \cdot [p \sin \alpha + \tilde{f} \cos \alpha] \tilde{S}_{\psi Y}(\xi, \eta) \quad (37a)$$

$$\hat{u} = \hat{G}_{uY} \tilde{Y}_0 \hat{F}_3(s) = \hat{F}_3(s) \beta(p) \tilde{Y}_0 \cdot [p \sin \alpha + \tilde{f} \cos \alpha] \hat{S}_{uY}(\xi, \eta) \quad (37b)$$

$$\hat{w} = \hat{G}_{wY} \tilde{Y}_0 \hat{F}_3(s) = \hat{F}_3(s) \beta(p) \tilde{Y}_0 \cdot [p \sin \alpha + \tilde{f} \cos \alpha] \hat{S}_{wY}(\xi, \eta) \quad (37c)$$

$$\hat{v} = \frac{1}{p} \left[\hat{F}_3(s) \hat{F}_1(\xi) \frac{\partial}{\partial \eta} \hat{F}_2(\eta) \tilde{Y}_0 \cos \alpha - \tilde{f} \hat{u} \right] = \frac{1}{p} \{ \tilde{Y}_0 \hat{F}_3(s) \hat{S}_{vY}(\xi, \eta) \cos \alpha - \tilde{f} \hat{u} \} \quad (37d)$$

$$\hat{b} = -\frac{1}{p} \tilde{N}^2 \hat{w} \quad (37e)$$

In (37) the $\hat{S}(\xi, \eta)$ functions describe the spatial structure in the nondimensional space of the corresponding variable. The $\hat{S}(\xi, \eta)$ are functions of p through ξ; therefore the $\hat{S}(\xi, \eta)$ functions are functions of time.

Through inverse Laplace transform, from (37), we have the time evolution

$$\tilde{\psi} = \tilde{Y}_0 \{ \tilde{G}_{\psi Y}(\xi, \eta, \tau) * \tilde{F}_3(\tau) \} \quad (38a)$$

$$\tilde{u} = \tilde{Y}_0 \{ \tilde{G}_{uY}(\xi, \eta, \tau) * \tilde{F}_3(\tau) \} \quad (38b)$$

$$\tilde{w} = \tilde{Y}_0 \{ \tilde{G}_{wY}(\xi, \eta, \tau) * \tilde{F}_3(\tau) \} \quad (38c)$$

$$\tilde{v} = \{ \exp(-\tilde{\lambda} \tau) * [\tilde{Y}_0 \tilde{F}_3(\tau) * \tilde{S}_{vY}(\xi, \eta) - \tilde{f} \tilde{u}] \} \quad (38d)$$

$$\tilde{b} = -\tilde{N}^2 \{ \exp(-\tilde{\lambda} \tau) * \tilde{w} \} \quad (38e)$$

where $\{\tilde{F}(\tau) * \tilde{G}(\tau)\}$ denotes a product in the Faltung theorem sense [*Fodor*, 1965]:

$$\{\tilde{F}(\tau) * \tilde{G}(\tau)\} = \int_0^{\tau} \tilde{G}(\tau - u) \tilde{F}(u)\, du \quad (39)$$

4.3. *Onset and Asymptotic Behavior*

The onset and the asymptotic behavior of the sea current can be studied using some properties of the Laplace transform.

The onset. When time t is small in comparison with the characteristic time scale T,

$$t \ll T = \frac{1}{(f^2 + \lambda^2)^{1/2}} \quad (40)$$

We can expand the stream function in a Taylor series near the time origin:

$$\tilde{\psi}(\xi, \eta, \tau) = \tilde{\psi}(\xi, \eta, \tau = 0) + \tau \frac{\partial}{\partial \tau} \tilde{\psi}(\xi, \eta, \tau = 0) + \frac{\tau^2}{2} \frac{\partial^2}{\partial \tau^2} \tilde{\psi}(\xi, \eta, \tau = 0) + \cdots \quad (41)$$

where

$$\tilde{\psi}(\xi, \eta, \tau = 0) = \lim_{s \to \infty} s \hat{\psi}$$

$$\frac{\partial}{\partial \tau} \tilde{\psi}(\xi, \eta, \tau = 0) = \lim_{s \to \infty} s^2 \hat{\psi}$$

$$\frac{\partial^2}{\partial \tau^2} \tilde{\psi}(\xi, \eta, \tau = 0) = \lim_{s \to \infty} s^3 \hat{\psi}$$

When we apply (41) to (37), we see that in $[p \sin \alpha + \tilde{f} \cos \alpha]$ the sine term prevails over the cosine term, i.e., at the onset, the offshore wind stress is more effective than the alongshore wind stress in driving the upwelling. Furthermore in (37) the $\hat{S}(\xi, \eta)$ functions are not functions of p; therefore $\tilde{S}(\xi, \eta)$ are not functions of time:

$$\tilde{S}(\xi, \eta) = \hat{S}(\xi, \eta) \quad (42)$$

with

$$\xi = \frac{x}{h} \qquad \eta = \frac{z}{h}$$

where

$$R = h \qquad A = 1 \quad (43b)$$

At the onset the system behaves nonhydrostatically, with an aspect ratio A equal to unity and a horizontal scale R equal to the vertical scale h.

The asymptotic solution. When the time t is much larger then the characteristic time T,

$$t \gg T = \frac{1}{(f^2 + \lambda^2)^{1/2}} \quad (44)$$

the sea current reaches its asymptotic state, which can be computed through the following limit:

$$\tilde{\psi}(\xi, \eta, \tau) = \lim_{s \to 0} s\hat{\psi} \tag{45}$$

When we apply (45) to (37), the factor $[p \sin \alpha + \tilde{f} \cos \alpha]$ becomes $[\lambda \sin \alpha + \tilde{f} \cos \alpha]$. Thus the amount of upwelling driven by the offshore wind stress is proportional to friction, and the amount of upwelling driven by the alongshore wind stress is proportional to inertia. In the asymptotic state, the structure functions $\tilde{S}(\xi, \eta)$ are not functions of time:

$$\tilde{S}^n(\xi, \eta) = \hat{S}^n(\xi, \eta) \tag{46}$$

with

$$\xi = \frac{x}{R} \qquad \eta = \frac{z}{h} \tag{47a}$$

where

$$R = \left(\frac{N^2 + \lambda^2}{f^2 + \lambda^2}\right)^{1/2} h \approx \frac{N}{(f^2 + \lambda^2)^{1/2}} h \qquad A = \frac{h}{R} \tag{47b}$$

The system behaves hydrostatically, with a horizontal scale equal to the Rossby radius R and with an aspect ratio A equal to the ratio between the vertical scale and the Rossby deformation radius.

We make use of (41) and (45) in section 5.1.

5. Sea Current Response to a Nonperiodic in Time Wind Stress

5.1. *Introduction*

In this section we examine the behavior of the sea current induced by a wind stress which has a constant intensity over an infinite or a finite fetch (i.e., (22) and (23)), with a vertical distribution given by (26). In general terms,

$$\hat{F}_1(\xi) \frac{\partial^2}{\partial \eta^2} \hat{F}_2(\eta) = \sum_{n=0}^{N} a_n He(\xi - \bar{l}_n)\delta(\eta + \bar{h}_n) \tag{48}$$

$$a_0 = 1 \qquad \bar{h}_0 = 1 \qquad \bar{l}_0 = 0$$

A large variety of wind stress distributions can be described with appropriate choices of a_n, $\bar{h}_n$, and $\bar{l}_n$. We can consider the wind stress as the sum of finite contributions of a_n intensity in the region defined by $\bar{l}_n < \xi < \bar{l}_{n+1}$ and $0 < \eta < \bar{h}_n$.

For instance, a horizontally uniform wind stress can be represented with

$$a_0 = 1 \qquad a_{n \geq 1} = 0 \qquad \bar{l}_0 = 0 \qquad \bar{h}_0 = 1 \tag{49}$$

a horizontally uniform wind stress over a finite region $\bar{l}_1$ can be represented with

$$\begin{aligned} &a_0 = 1 \qquad a_1 = -1 \qquad a_{n \geq 2} = 0 \\ &\bar{l}_0 = 0 \qquad \bar{l}_1 \neq 0 \qquad \bar{h}_0 = \bar{h}_1 = 1 \end{aligned} \tag{50}$$

Using (34), we can compute the transfer function for the wind stress spatial distribution given in (48):

$$\hat{G}_{\psi Y}(\xi, \eta, s) = \beta(p)[p \sin \alpha + \tilde{f} \cos \alpha] \sum_{n=0}^{N} a_n \hat{S}^n_{\psi Y}(\xi, \eta) \tag{51a}$$

$$\hat{G}_{uY}(\xi, \eta, s) = \beta(p)[p \sin \alpha + \tilde{f} \cos \alpha] \sum_{n=0}^{N} a_n \hat{S}^n_{uY}(\xi, \eta) \tag{51b}$$

$$\hat{G}_{wY}(\xi, \eta, s) = \beta(p)[p \sin \alpha + \tilde{f} \cos \alpha] \sum_{n=0}^{N} a_n \hat{S}^n_{wY}(\xi, \eta) \tag{51c}$$

$$\hat{G}_{vY}(\xi, \eta, s) = \frac{1}{p} \cos \alpha \sum_{n=0}^{N} a_n \hat{S}^n_{vY}(\xi, \eta) - \tilde{f} \hat{G}_{uY}(\xi, \eta, s) \Big] \tag{51d}$$

$$\hat{G}_{bY}(\xi, \eta, s) = -\frac{N^2}{p} \hat{G}_{wY}(\xi, \eta, s) \tag{51e}$$

The structure functions $\tilde{S}^n$ in (51), associated with the forcing specified in (48), are given in Appendix C.

5.2. *The Onset, the Transient, and the Asymptotic Behavior of the Sea Current*

The onset. When time t is small, we can use the Taylor expansion given in (41) for the different fields. For a δ wind impulse (equation (27)), we have

$$\psi = T\Upsilon_0[\sin \alpha + ft \cos \alpha] \sum_{n=0}^{N} a_n \tilde{S}^n_{\psi Y}(\xi, \eta)$$

$$\approx T\Upsilon_0 \sin \alpha \sum_{n=0}^{N} a_n \tilde{S}^n_{\psi Y}(\xi, \eta) \tag{52a}$$

$$u = \frac{T}{h} \Upsilon_0[\sin \alpha + ft \cos \alpha] \sum_{n=0}^{N} a_n \tilde{S}^n_{uY}(\xi, \eta)$$

$$\approx \frac{T}{h} \Upsilon_0 \sin \alpha \sum_{n=0}^{N} a_n \tilde{S}^n_{uY}(\xi, \eta) \tag{52b}$$

$$w = \frac{T}{h} \Upsilon_0[\sin \alpha + ft \cos \alpha] \sum_{n=0}^{N} a_n \tilde{S}^n_{wY}(\xi, \eta)$$

$$\approx \frac{T}{h} \Upsilon_0 \sin \alpha \sum_{n=0}^{N} a_n \tilde{S}^n_{wY}(\xi, \eta) \tag{52c}$$

$$v = \frac{\Upsilon_0}{h} t \cos \alpha \sum_{n=0}^{N} a_n \tilde{S}^n_{vY}(\xi, \eta) - f t \sin \alpha + \frac{1}{2!} t^2 f \cos \alpha \sum_{n=0}^{N} a_n \tilde{S}^n_{uY}(\xi, \eta)$$

$$\frac{t}{h} \Upsilon_0 \sum_{n=0}^{N} a_n[\cos \alpha \tilde{S}^n_{vY}(\xi, \eta) + \sin \alpha \tilde{S}^n_{uY}(\xi, \eta)] \tag{52d}$$

$$b = -N^2 \frac{T}{h} \Upsilon_0 \left[t \sin \alpha + \frac{1}{2!} t^2 f \cos \alpha \right]$$

$$\sum_{n=0}^{N} a_n \tilde{S}^n_{w\Upsilon}(\xi, \eta) \approx 0 \qquad (52e)$$

The onset response to a Heaviside wind impulse (equation (28)) is the time integral of (52), and the onset response to a linearly growing wind impulse (equation (30)) equals (52) integrated in time twice, and so on. The response, for any wind impulse, can be reconstructed by expanding the impulse in a Taylor series near the time origin, then using the properties illustrated above.

Initially, for a time duration small in comparison to the characteristic time $t \ll T$ and for any impulse of the wind stress, the major contribution to the upwelling comes from the offshore wind stress and not from the alongshore wind stress, which is higher order in time (see equation (52)).

Furthermore, from (52) we see that in the initial stages the contribution of the alongshore wind stress to the stream function ψ, to the offshore current u, and to the upwelling w is negligible, and that only the offshore wind stress contributes.

The offshore wind stress through the Coriolis term and the alongshore wind stress equally contribute to the alongshore current v. The alongshore wind stress contribution, through the Coriolis term, is negligible. The perturbations of the buoyancy b due to the vertical advection are initially small.

The spatial structure functions $\tilde{S}^n(\xi, \eta)$ are

$$\tilde{S}^n(\xi, \eta) = \hat{S}^n(\xi, \eta) \qquad (53)$$

with

$$\xi = \frac{x}{h} \qquad \eta = \frac{z}{h}$$

where the form of $\hat{S}^n(\xi, \eta)$ is given in Appendix C. In section 4.3 we saw that at the onset the system behaves nonhydrostatically, with an aspect ratio A equal to unity and that the overturning occurs in a horizontal region $R = h$, i.e., (43).

For a horizontally uniform wind stress (equation (49)) the maximum intensity of the upwelling in a very deep sea occurs when $\eta^2 = 1 + \xi^2$, i.e., at a depth

$$z = -h \left[1 + \left(\frac{x}{h} \right)^2 \right]^{1/2}$$

In an infinite deep sea, the maximum intensity of the upwelling near the coast ($x = 0$) occurs at the depth where the action of the wind stress vanishes, i.e., $z = -h$. The maximum occurs at larger depths away from the coast (i.e., $x > 0$), and the intensity decreases to zero for $x \gg R = h$.

In a sea of finite depth H, the maximum intensity of the upwelling occurs where the following relation between the horizontal coordinate and the vertical coordinate is fulfilled:

$$\cos \pi \frac{z}{H} \cosh \pi \frac{x}{H} = \cos \pi \frac{h}{H}$$

The transient. When the time t is comparable with T, to see how the sea current goes from its initial state to its asymptotic state, we have to Laplace invert the transfer functions $\hat{G}_\Upsilon(\xi, \eta, s)$ in (51). Since the system is nonhydrostatic only in the initial stage, we make the hydrostatic approximation. The vertical velocity is

$$w = u_0 \frac{h}{R} \{ \tilde{F}_3(\tau) * \tilde{G}_{w\Upsilon}(\xi, \eta, \tau) \} \qquad (54)$$

The time dependent transfer function $\tilde{G}_\Upsilon(\xi, \eta, \tau)$ for a sea of infinite depth is

$$\tilde{G}_{w\Upsilon}(\xi, \eta, \tau) = \exp(-\tilde{\lambda}\tau) \left\{ \sin(\tilde{f}\tau + \alpha) * \sum_{n=0}^{N} a_n \tilde{G}^n_w \right\}$$

The $\tilde{G}^n_w(\xi, \eta, \tau)$ functions are

$$\tilde{G}^n_w(\xi, \eta, \tau) = \tilde{H}^n_w(\xi, \eta, \tau) - \tilde{f}\tilde{F}^n_w(\xi, \eta, \tau)$$

$$\tilde{H}^n_w = \frac{1}{2\pi} \frac{1}{\tau} \left\{ \left[\cos \frac{n_+}{\xi_-} \tau - \cos \frac{\eta_-}{\xi_-} \tau \right] + \left[\cos \frac{\eta_+}{\xi_+} \tau - \cos \frac{\eta_-}{\xi_+} \tau \right] \right\}$$

$$\tilde{F}^n_w = \frac{1}{2\pi} \frac{1}{\tau} \left[\frac{\sin \nu_{-++}\tau \sin \nu_{-+-}\tau}{(\nu_{-++}\nu_{-+-})^{1/2}} \right.$$

$$\left. \frac{\sin \nu_{--+}\tau \sin \nu_{---}\tau}{(\nu_{--+}\nu_{---})^{1/2}} \right] + \frac{1}{2\pi}$$

$$\left[\frac{\sin \nu_{+++}\tau \sin \nu_{++-}\tau}{} - \frac{\sin \nu_{--+}\tau \sin \nu_{---}\tau}{(\nu_{+-+}\nu_{+--})^{1/2}} \right]$$

$$\eta = \frac{z}{h} \qquad \xi = \frac{x}{R} \qquad \tau = t(f^2 + \lambda^2)^{1/2}$$

$$\xi_+ = (\xi + \tilde{l}_n) \qquad \xi_- = (\xi - \tilde{l}_n) \qquad \eta_+ = (\eta + \tilde{h}_n)$$

$$\eta_- = (\eta - \tilde{h}_n)$$

$$\nu_{+++} = \frac{1}{2} \left\{ \left[\tilde{f}^2 + \left(\frac{\eta_+}{\xi_+} \right)^2 \right]^{1/2} + \frac{\eta_+}{\xi_+} \right\}$$

$$\nu_{++-} = \frac{1}{2} \left\{ \left[\tilde{f}^2 + \left(\frac{\eta_+}{\xi_+} \right)^2 \right]^{1/2} \frac{\eta_+}{\xi_+} \right\}$$

$$\nu_{+-+} = \frac{1}{2} \left\{ \left[\tilde{f}^2 + \left(\frac{\eta_-}{\xi_+} \right)^2 \right]^{1/2} + \frac{\eta_-}{\xi_+} \right\}$$

$$\nu_{+--} = \frac{1}{2} \left\{ \left[\tilde{f}^2 + \left(\frac{\eta_-}{\xi_+} \right)^2 \right]^{1/2} \frac{\eta_-}{\xi_+} \right\}$$

$$\nu_{-++} = \frac{1}{2} \left\{ \left[\tilde{f}^2 + \left(\frac{\eta_+}{\xi_-} \right)^2 \right]^{1/2} + \frac{\eta_+}{\xi_-} \right\}$$

$$\nu_{-+-} = \frac{1}{2} \left\{ \left[\tilde{f}^2 + \left(\frac{\eta_+}{\xi_-} \right)^2 \right]^{1/2} \frac{\eta_+}{\xi_-} \right\}$$

$$\nu_{--+} = \frac{1}{2} \left\{ \left[\tilde{f}^2 + \left(\frac{\eta_-}{\xi_-} \right)^2 \right]^{1/2} + \frac{\eta_-}{\xi_-} \right\}$$

$$\nu_{---} = \frac{1}{2} \left\{ \left[\tilde{f}^2 + \left(\frac{\eta_-}{\xi_-} \right)^2 \right]^{1/2} \frac{\eta_-}{\xi_-} \right\}$$

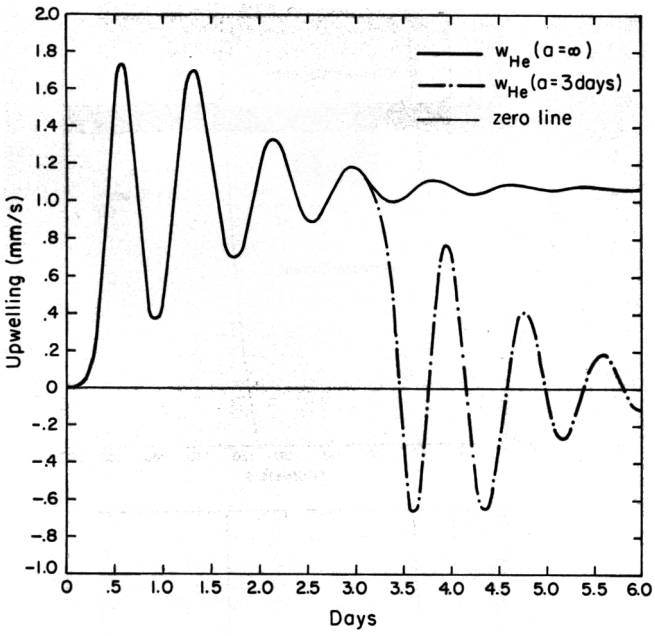

Fig. 1. Time evolution of the upwelling intensity at the coordinate point ($x = 0.1R$, $z = -0.9h$). The e-folding time λ^{-1} has been set equal to 1 day. The solid line shows the upwelling behavior for an abrupt wind impulse; the oscillations are due to the inertia-gravity waves, and the asymptotic state is reached when $t \approx 3\lambda^{-1}$. The dashed line shows how the system reacts if the wind impulse ceases after 3 days; the upwelling intensity goes to zero through a series of damped inertia-gravity waves for $t > 3\lambda^{-1}$.

The upwelling goes from its initial state to the asymptotic state through a series of damped inertial gravity waves. Figure 1 shows the transition behavior from rest to the asymptotic value of the upwelling intensity, close to the coast, forced by an alongshore wind stress. The damping is essentially due to friction. When the wind impulse ceases, the intensity of the upwelling goes to zero through a number of inertial gravity oscillations which depend on latitude and friction. *Salat et al.* [1989] have observed a number of inertial oscillations induced by an impulse of offshore wind in the northwestern Mediterranean Sea, near the Spanish coast.

The asymptote. When the time t is much larger than the characteristic time T, the asymptotic state of the sea current can be computed through the limit given by (45). The asymptotic intensity of the sea current is eventually zero when the wind stress forcing acts for a limited time; the system eventually diverges if an indefinitely growing forcing is applied. In the case of finite amplitude forcing the sea current reaches a finite asymptotic value, where the contribution of the offshore wind stress to the stream function ψ, to the onshore current u, and to the upwelling w depends on friction. The contribution of the alongshore wind stress to the stream function ψ, to the onshore current u, and to the upwelling w depends on inertia. The offshore wind stress, through the inertial term, and the alongshore wind stress equally contribute to the alongshore current v. Actually the offshore wind stress contribution, relative to the alongshore wind contribution, prevails in the early stage and then becomes proportional to λ/f in the mature stage. The perturbations of the buoyancy b due to the vertical advection and to the diabatic term are of the same order.

For a Heaviside impulse of wind, we have

$$\psi = u_0 h[\tilde{\lambda} \sin\alpha + \tilde{f}\cos\alpha] \sum_{n=0}^{N} a_n \tilde{S}^n_{\psi Y}(\xi, \eta)$$

$$u = u_0[\tilde{\lambda} \sin\alpha + \tilde{f}\cos\alpha] \sum_{n=0}^{N} a_n \tilde{S}^n_{uY}(\xi, \eta)$$

$$w = u_0 \frac{h}{R}[\tilde{\lambda} \sin\alpha + \tilde{f}\cos\alpha] \sum_{n=0}^{N} a_n \tilde{S}^n_{wY}(\xi, \eta)$$

$$v = \frac{1}{\tilde{\lambda}}\left\{ u_0 \cos\alpha \sum_{n=0}^{N} a_n \tilde{S}^n_{vY}(\xi, \eta) - \tilde{f}u \right\}$$

$$b = \frac{T^2 N^2}{\lambda}$$

The spatial structure functions $\tilde{S}^n(\xi, \eta)$ are

$$\tilde{S}^n(\xi, \eta) = \hat{S}^n(\xi, \eta) \tag{56}$$

where the $\hat{S}^n(\xi, \eta)$ functions are given in Appendix C, where $\xi = x/R$, $\eta = z/h$, and $R = h[N/(f^2 + \lambda^2)^{1/2}]$.

From section 4.3, we see that the asymptotic system behaves hydrostatically, with an aspect ratio equal to the ratio between the vertical scale h and the Rossby deformation radius R modified by the friction, and that the upwelling occurs in a region of horizontal extent equal to R.

For a horizontally uniform wind stress (equation (22)) the upwelling is given by

$$w = u_0 \frac{h}{R}[\tilde{\lambda} \sin\alpha + \tilde{f}\cos\alpha] 2\tilde{S}_w \tag{57}$$

$$\tilde{S}_w = \frac{-}{2\pi} \ln\left[\frac{h^2x^2 + R^2(z+h)^2}{h^2x^2 + R^2(z-h)^2}\right]^{1/2}$$

Thus $\tilde{S}_w$ vanishes when $\xi > 1$, i.e., the upwelling is negligible when the distance from the coast is larger than the Rossby deformation radius R. The maximum intensity of the upwelling in a very deep sea occurs when

$$z = -h\left[\quad \left(\frac{x}{R}\right)^2\right]^{1/}$$

In an infinite deep sea, the maximum intensity of the upwelling occurs at $z = h$ near the coast (i.e., $x = 0$), and deeper in the ocean far from the coast.

In a sea of finite depth H, the maximum intensity of the upwelling occurs where the following relation between the horizontal coordinate and the vertical coordinate is fulfilled:

$$\cos\pi\frac{z}{H}\cosh\pi\frac{h}{H}\frac{x}{R} = \cos\pi\frac{h}{H}$$

Figure 2 shows the vertical structure of the upwelling for a sea of infinite depth and for a sea of finite depth. When $H < 2h$, the horizontal scale of the upwelling is reduced by the shallowness of the sea, and the maximum intensity of the upwelling is reduced and occurs at lower depth than in an infinitely deep sea (for $x > 0$).

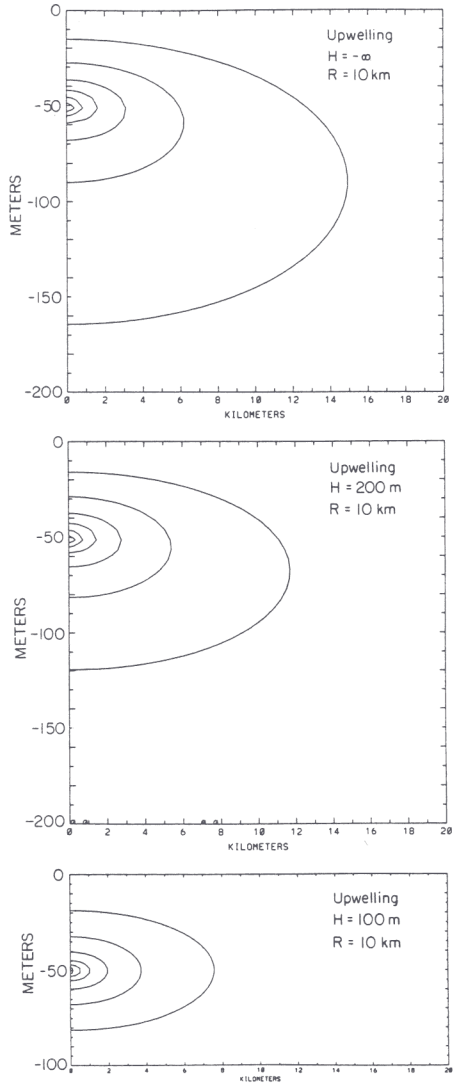

Fig. 2. Asymptotic upwelling isolines, $\Delta w = 0.2$ mm/s, for an infinitely deep sea, for a 200-m-deep sea, and for a 100-m-deep sea, respectively. The Rossby deformation radius R has been set equal to 10 km. The maximum intensity occurs near the coast for $z = h$; away from the coast the peak of the upwelling intensity occurs at a greater depth in an infinitely deep sea.

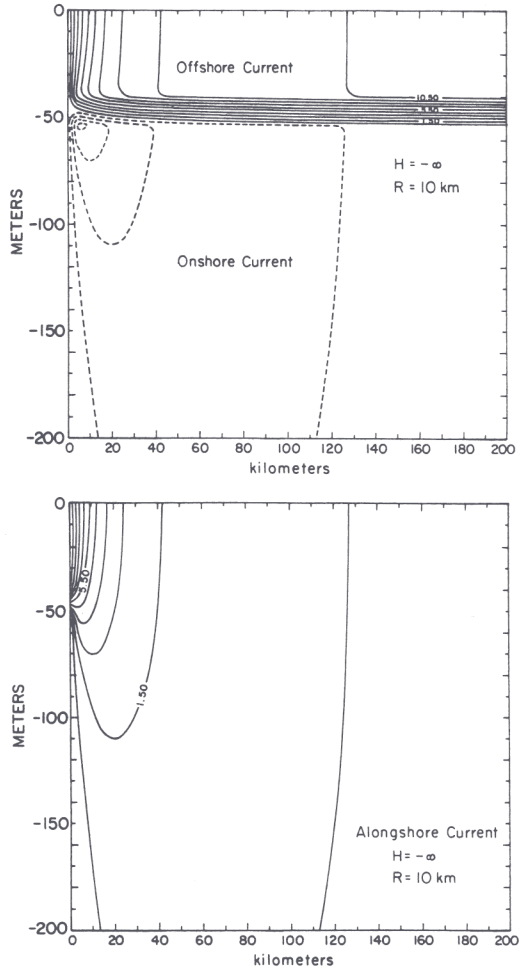

Fig. 3. Isolines of the asymptotic offshore and alongshore current, respectively ($\Delta u = 1$ cm/s and $\Delta v = 1$ cm/s), in an infinitely deep sea with a Rossby deformation radius R equal to 10 km and when the friction is equal to the inertia of the system, i.e., $\lambda = f$. The offshore current is close to the surface and as deep as the depth of the stress; its intensity is zero at the coast and increases to its asymptotic value for $x \gg R$. The return flow below the surface layer is much deeper and weaker than the surface flow. The alongshore current shows an intense jet close to the coast in the region $0 < x < R$.

Figure 3 shows the corresponding offshore and alongshore currents. Near the surface the flow is offshore with increasing intensity away from the coast; the intensity reaches its asymptotic value after one Rossby deformation radius. The return flow is much weaker and occurs in a much deeper layer. The alongshore current shows a marked jet near the coast within the distance of one Rossby deformation radius. For a horizontally uniform wind stress (equation (22)) the offshore current is given by

$$u = u_0[\tilde{\lambda} \sin \alpha + \tilde{f} \cos \alpha]2\tilde{S}_u$$
$$\tilde{S}_u = \frac{1}{2\pi}\left[\tan^{-1}\frac{hx}{R(z+h)} - \tan^{-1}\frac{hx}{R(z-h)}\right] \tag{58}$$

Near the coast ($0 < x < R$),

$$\tilde{S}_u \approx \frac{1}{\pi}\frac{x}{R}\frac{h^2}{h^2 - z^2} \qquad z \neq -h$$

i.e., near the coast, the offshore current is sheared with increasing intensity and shear for increasing distance from the coast. Far from the coast ($x > R$),

$$\tilde{S}_u \lesssim \tfrac{1}{2} \qquad -h < z < 0$$

$$\tilde{S}_u \lesssim 0 \qquad -h < z < -\infty$$

i.e., at a distance from the coast larger than the Rossby radius, the shear is concentrated in a narrow region around $z \approx -h$; the offshore current is almost constant through the mixed layer and is negative but weak below it.

The alongshore current is the difference between the current directly driven by the alongshore wind stress, which has the shear concentrated around $z \approx -h$, and the current connected to the sheared offshore current through inertia (equation (55d)). The two contributions have their maximum difference for $0 < x < R$, giving the alongshore coastal jet, and almost cancel for $x \gg R$ (Figure 3).

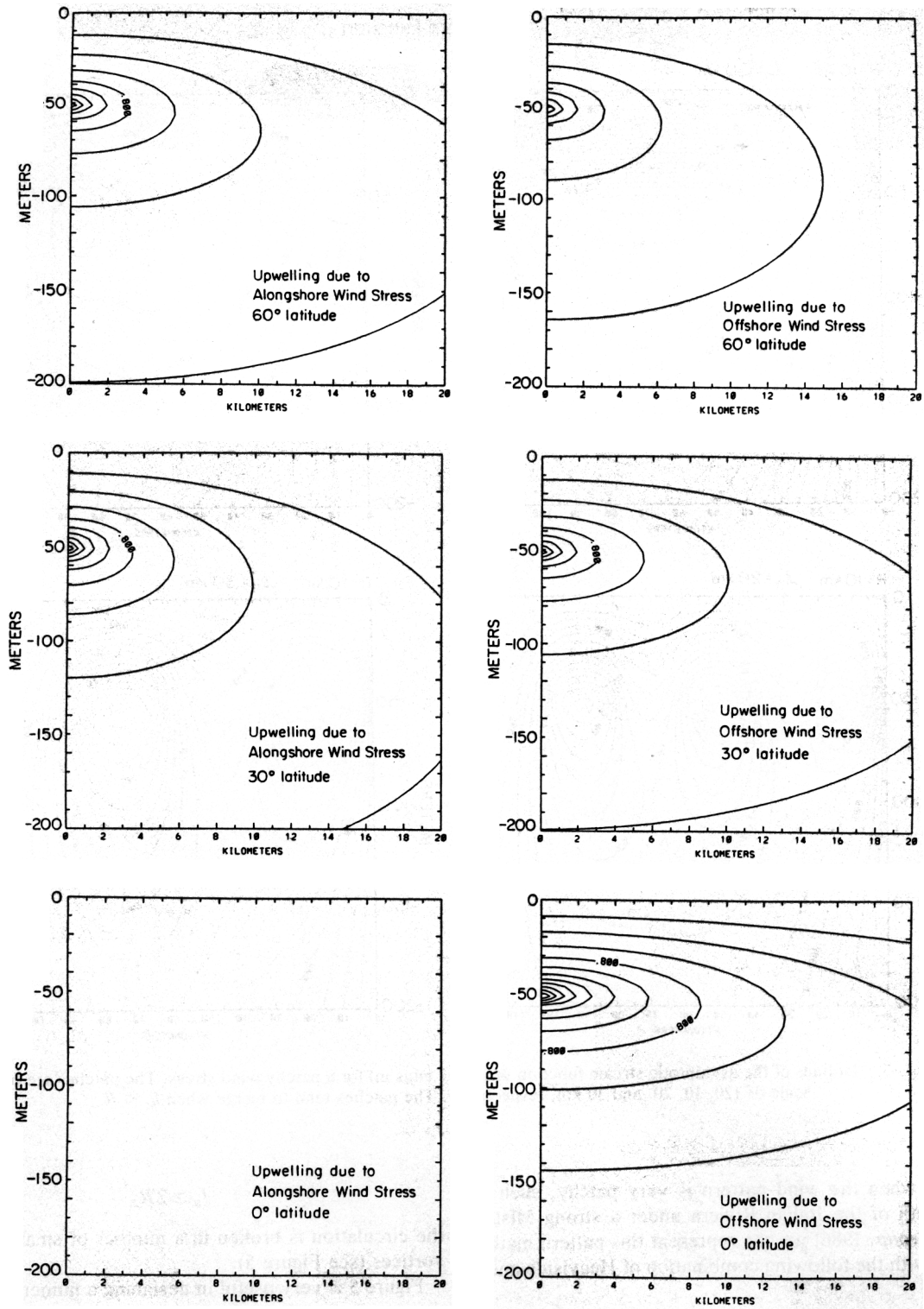

Fig. 4. Isolines of the asymptotic upwelling (Δw = 0.2 mm/s), forced by the alongshore wind stress and by the offshore wind stress, respectively, at 0°, 30°, 60° of latitude ($\lambda = f$) in an infinite deep sea. The action of the alongshore wind stress on the upwelling occurs through inertia; the offshore wind stress acts on the upwelling through friction.

Figure 4 shows the upwelling due to the offshore and the alongshore wind stress. The intensity of the upwelling due to the alongshore wind stress increases with increasing latitude, while the horizontal scale decreases. The intensity of the upwelling due to the offshore wind stress decreases with increasing latitude. The contribution of the offshore wind stress to the upwelling is proportional to friction, and the contribution of the alongshore wind stress is proportional to inertia (see (55)); the friction λ has been assumed of the same order as f.

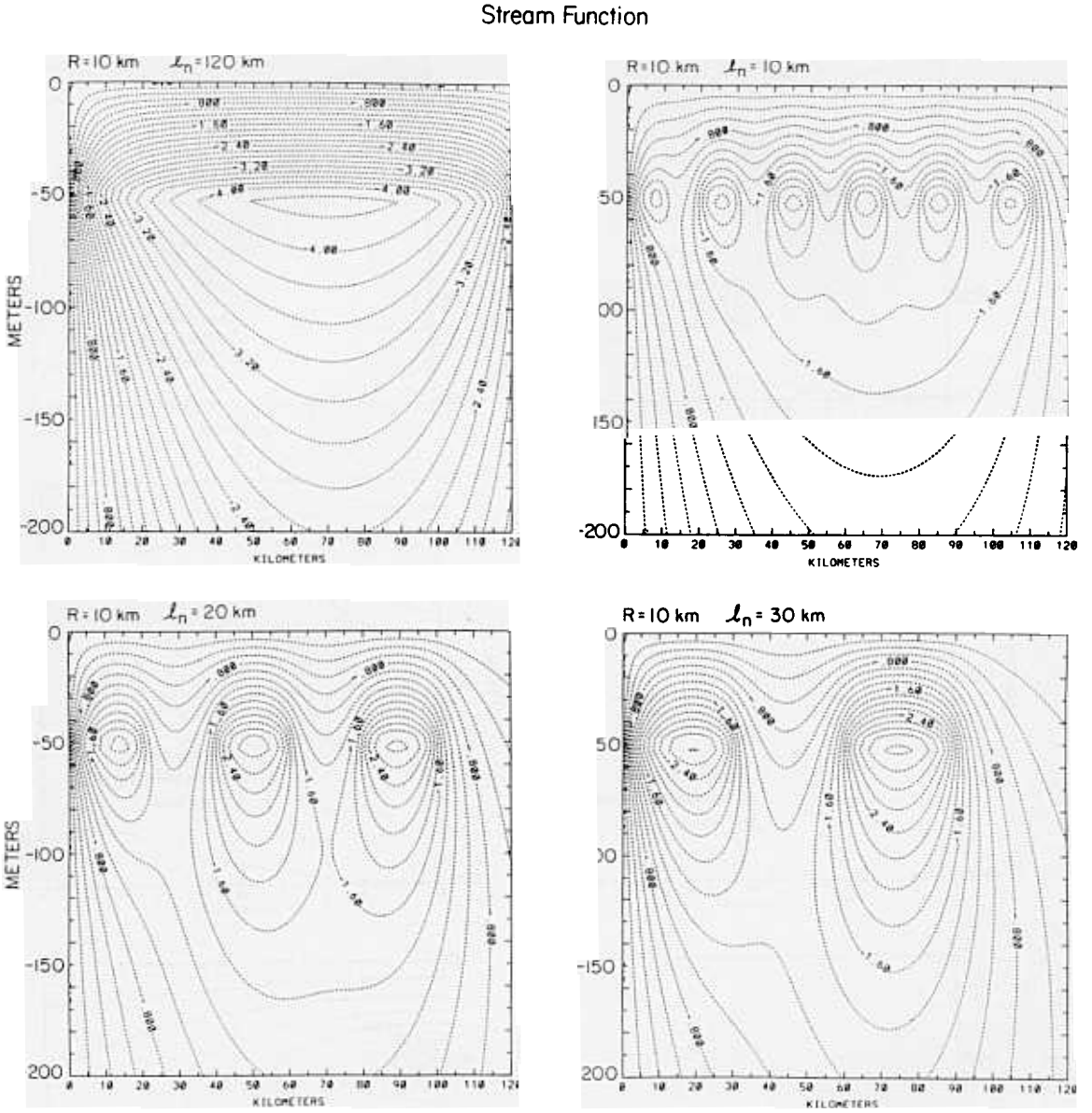

Fig. 5. Isolines of the asymptotic stream function $\psi(\Delta\psi = 2$ cm/s m) for a patchy wind stress. The patches are of the scale of 120, 10, 20, and 30 km, respectively. The patches tend to merge when $l_n < R$.

Finally, when the wind pattern is very patchy, such as occurs south of the Italian Riviera under a strong Mistral [*ALPEX Group*, 1986] we can represent this pattern mathematically with the following combination of Heaviside and δ functions:

$$\hat{F}_1(\xi)\frac{\partial^2}{\partial\eta^2}\hat{F}_2(\eta) = \sum_{n=0}^{2M+1} -1)^n He(\xi - \bar{l}_n)\delta(\eta + \bar{h}_n) \qquad (59)$$

The stream function for this situation (Figure 5) shows that when

$$l_n < 2R_n \qquad R_n = \frac{N}{(f^2 + \lambda^2)^{1/2}} h_n$$

the wind stress induces one coherent vortex. Conversely when

$$l_n > 2R_n$$

the circulation is broken in a number of small independent vortices (see Figure 5).

Figure 5 is very useful in designing a numerical model for the description of the dynamics of the coastal waters, i.e., a horizontal resolution R is needed when there are horizontal inhomogeneities of the wind stress $l_n \leq R_n$; the flow will smooth the inhomogeneities for $l_n \ll R_n$. A finer resolution than $R_{n=0}$ is required near the coast in order to resolve the upwelling region (Figure 2) and the coastal jet (Figure 3).

6. Region of the Upwelling Can Exceed the Rossby Deformation Radius

In this section we examine the behavior of upwelling when the wind stress is not horizontally uniform within finite

regions. We discuss the case when the wind stress is linearly increasing up to $\tilde{l}$ and then linearly decreasing up to $2\tilde{l}$, such as occurs along the coast of southern California [*Winant et al.*, 1988]. The vertical velocity for the forcing specified in (24) is

$$w = u_0 \frac{h}{R} [\tilde{\lambda} \sin \alpha + \tilde{f} \cos \alpha](\tilde{S}_w^1 + \tilde{S}_w^2) \tag{60}$$

$\tilde{S}_w^1$ gives the contribution of the increasing part of the wind stress, while $\tilde{S}_w^2$ gives the contribution of the decreasing part of the wind stress.

In (60) the $\tilde{S}_w^1$ function is

$$\tilde{S}_w^1 = -\frac{1}{2\pi}\frac{\xi}{\tilde{l}} \ln \left[\frac{\xi_-^2 + \eta_-^2}{\xi_-^2 + \eta_+^2}\frac{\xi_+^2 + \eta_+^2}{\xi_+^2 + \eta_-^2}\right]^{1/2} - \frac{1}{2\pi}\frac{\eta_+}{\tilde{l}}\left[\tan^{-1}\frac{\xi_+}{\eta_+} - \tan^{-1}\frac{\xi_-}{\eta_+}\right] - \frac{1}{2\pi}\frac{\eta_-}{\tilde{l}}\left[\tan^{-1}\frac{\xi_-}{\eta_-} - \tan^{-1}\frac{\xi_+}{\eta_-}\right]$$

$\tilde{S}_w^1$ vanishes when $x > l + R$; the $\tilde{S}_w^2$ function in (60) is

$$\tilde{S}_w^2 = -\frac{1}{2\pi}\left\{\frac{\xi_{--}}{\tilde{l}} \ln \left[\frac{\xi_{--}^2 + \eta_+^2}{\xi_-^2 + \eta_+^2}\frac{\xi_-^2 + \eta_-^2}{\xi_{--}^2 + \eta_-^2}\right]^{1/2} + \frac{\xi_{++}}{\tilde{l}} \ln \left[\frac{\xi_{++}^2 + \eta_-^2}{\xi_+^2 + \eta_-^2}\frac{\xi_+^2 + \eta_+^2}{\xi_{++}^2 + \eta_+^2}\right]^{1/2}\right\} + \frac{1}{2\pi}\frac{\eta_+}{\tilde{l}}\left[\tan^{-1}\frac{\xi_{--}}{\eta_+} - \tan^{-1}\frac{\xi_-}{\eta_+} + \tan^{-1}\frac{\xi_+}{\eta_+} - \tan^{-1}\frac{\xi_{++}}{\eta_+}\right] + \frac{1}{2\pi}\frac{\eta_-}{\tilde{l}}\left[\tan^{-1}\frac{\xi_{++}}{\eta_-} - \tan^{-1}\frac{\xi_+}{\eta_-} + \tan^{-1}\frac{\xi_-}{\eta_-} - \tan^{-1}\frac{\xi_{--}}{\eta_-}\right]$$

$\tilde{S}_w^2$ vanishes when $x > 2l + R$. Here

$$\eta = \frac{z}{h} \qquad \xi = \frac{x}{h}\frac{(f^2 + \lambda^2)^{1/2}}{N}$$

$$\xi_+ = (\xi + \tilde{l}) \qquad \xi_- = (\xi - \tilde{l}) \qquad \xi_{++} = (\xi + 2\tilde{l})$$

$$\xi_{--} = (\xi - 2\tilde{l}) \qquad \eta_+ = (\eta + \tilde{h}) \qquad \eta_- = (\eta - \tilde{h})$$

Comparison between Figure 6 (equation (60)) and Figure 2 (equation (57)) shows that the extension of the upwelling is greatly increased by a linearly increasing wind stress. In fact for a horizontally uniform wind stress (equation (22)) the upwelling is negligible when the distance from the coast is larger than the Rossby deformation radius R (equation (57)).

For the forcing specified in (25), a finite fetch with decreasing and then increasing wind stress, the roles of the functions $\tilde{S}_w^1$ and $\tilde{S}_w^2$ are exchanged, i.e., $\tilde{S}_w^1$ is shifted horizontally by l, and $\tilde{S}_w^2$ is shifted horizontally by $-l$; the result is that the coastal upwelling extends less than one Rossby deformation radius.

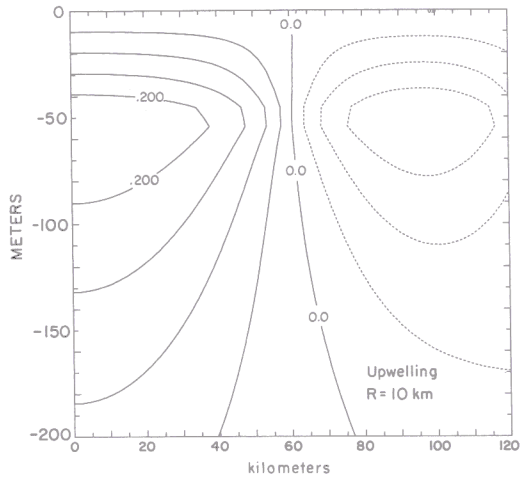

Fig. 6. Isolines of the asymptotic upwelling ($\Delta w = 0.05$ mm/s), forced by a wind stress increasing up to 60 km, and decreasing from 60 to 120 km. The upwelling occurs in a horizontal region larger than the Rossby deformation radius.

7. Sea Current Forced by Periodic Wind Stress

This case is relevant for the situation of several days of sea-land breezes [*Rotunno*, 1983; *Niino*, 1987]. In general, the sea current response to a periodic wind stress is found as a product, according to the Faltung theorem [*Fodor*, 1965] of the transfer functions $\tilde{G}$ and the forcing $\tilde{F}_3$ (equation (31)). Because of the time structure of the transfer function (curve A in Figure 1), a pure periodic behavior is reached only after a time which is a few times T; the transient disappears for $t > 3\lambda^{-1}$. We examine the asymptotic behavior of the sea current under the periodic wind stress:

$$\tilde{F}_1(\xi)\tilde{F}_2(\eta)\tilde{F}_3(\tau) = He(\xi)(\eta + 1)\left[\left(\frac{\partial}{\partial\tau} + \tilde{\lambda}\right) \sin \tilde{\omega}\tau + \tilde{f} \cos \tilde{\omega}\tau\right] = He(\xi)(\eta + 1)[(\tilde{\omega} + \tilde{f}) \cos \tilde{\omega}\tau + \tilde{\lambda} \sin \tilde{\omega}\tau] \tag{61}$$

This gives the result that, under periodic forcing, with no friction, the alongshore and the offshore wind stress both contribute in phase to the strength of the sea current.

7.1. *The Sea Current Behavior When* $f^2 + \lambda^2 - \omega^2 > 0$

Recalling that the cosine is the real part of the exponential with an imaginary argument and that the sine is its imaginary part, we pose

$$\tilde{\psi} = \tilde{\psi}_r + i\tilde{\psi}_i \tag{62}$$

Using (62), we can equate the real and imaginary parts separately. We then have two equations in nondimensional form.

The first equation is in phase with the cosine,

$$\frac{\partial^2}{\partial \xi^2}\tilde{\psi}_r + \frac{\partial^2}{\partial \eta^2}\tilde{\psi}_r - \Upsilon\left\{\frac{\partial^2}{\partial \zeta^2}\tilde{\psi}_i + \frac{\partial^2}{\partial \eta^2}\tilde{\psi}_i\right\}$$

$$= \beta_{\tilde{\omega}}\hat{\Upsilon}_0[\tilde{\omega} + \tilde{f}]He(\xi)\delta(\eta + 1 \quad (63)$$

and the second equation is in phase with the sine,

$$\frac{\partial^2}{\partial \xi^2}\tilde{\psi}_i + \frac{\partial^2}{\partial \eta^2}\tilde{\psi}_i + \Upsilon\left\{\frac{\partial^2}{\partial \zeta^2}\tilde{\psi}_r + \frac{\partial^2}{\partial \eta^2}\tilde{\psi}_r\right\}$$

$$= \beta_{\tilde{\omega}}\hat{\Upsilon}_0\tilde{\lambda}He(\xi)\delta(\eta + 1 \quad (64)$$

with

$$\beta_{\tilde{\omega}} = \frac{}{\tilde{f}^2 + \tilde{\lambda}^2 - \tilde{\omega}^2}$$

$$\xi = \alpha\frac{x}{h} = \alpha\zeta \qquad \zeta = \frac{x}{h}$$

$$\left(\frac{\tilde{f}^2 + \tilde{\lambda}^2 - \tilde{\omega}^2}{\tilde{N}^2 + \tilde{\lambda}^2 - \tilde{\omega}^2}\right)^{1/2} \approx \frac{(f^2 + \tilde{\lambda}^2 - \tilde{\omega}^2)^{1/2}}{\tilde{N}} = O(10^{-2})$$

$$\gamma = \frac{2\tilde{\omega}\tilde{\lambda}}{\tilde{f}^2 + \tilde{\lambda}^2 - \tilde{\omega}^2} = O(1) \quad (65)$$

Then we define

$$\tilde{\psi}_i^*\left(\frac{\xi}{\alpha}, \eta\right) = \gamma\tilde{\psi}_i \qquad \tilde{\psi}_r^*\left(\frac{\xi}{\alpha}, \eta\right) = \gamma\tilde{\psi}_r$$

$$\tilde{\psi}_c(\xi, \eta) = \tilde{\psi}_r - \tilde{\psi}_i^* \qquad \tilde{\psi}_s(\xi, \eta) = \tilde{\psi}_i + \tilde{\psi}_r^* \quad (66)$$

The out-of-phase contribution $\tilde{\psi}^*$ to the stream function has an amplitude factor equal to Υ, which decreases as friction decreases. The factor α in the horizontal coordinate, in the out-of-phase stream function $\tilde{\psi}^*$, confines the corresponding contribution (and the phase lag) to a region which is typically 2 orders of magnitude smaller than the Rossby deformation radius. Thus the out-of-phase stream function can be neglected in practical applications.

We can rewrite (63) and (64); for the stream function in-phase with the cosine,

$$\frac{\partial^2}{\partial \xi^2}\tilde{\psi}_c + \frac{\partial^2}{\partial \eta^2}\tilde{\psi}_c = \beta_{\tilde{\omega}}\hat{\Upsilon}_0[\tilde{\omega} + \tilde{f}]He(\xi)\delta(\eta + 1) \quad (67)$$

and for the stream function in phase with the sine,

$$\frac{\partial^2}{\partial \xi^2}\tilde{\psi}_s + \frac{\partial^2}{\partial \eta^2}\tilde{\psi}_s = \beta_{\tilde{\omega}}\hat{\Upsilon}_0\tilde{\lambda}He(\xi)\delta(\eta + 1) \quad (68)$$

Equations (67) and (68) are formally equal to (8), which we have already extensively studied. In (6) and (8), periodicity enhances the amplitude $\beta_{\tilde{\omega}}$ and the horizontal scale of motion R.

7.2. *Waves Generated by a Periodic Wind Stress When $\omega^2 - (f^2 + \lambda^2) > 0$*

The governing equation for the stream function has a hyperbolic term and an elliptical term. Sufficiently far from the coast (or when friction is small), the contribution coming from the elliptic term can be neglected. The propagating wave part of the perturbation can be described by the following hyperbolic equation:

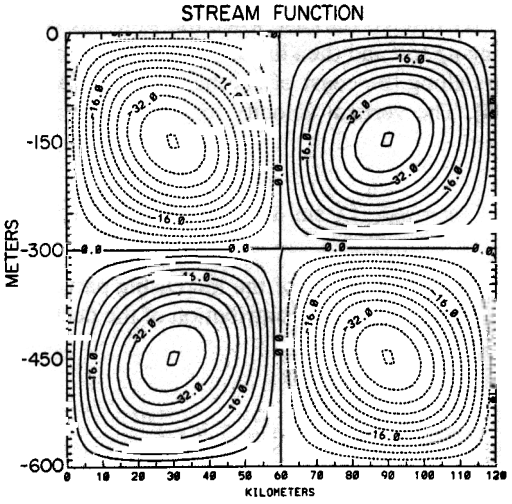

Fig. 7. Wave structure of the isolines of the stream function ψ under periodic forcing at low latitude. The wind stress forcing is confined to the first 60 km off the coast. Propagating waves are excited in the ocean by a periodic wind stress when $\omega^2 - (f^2 + \lambda^2) > 0$.

$$\frac{\partial^2}{\partial \xi^2}\tilde{\psi} - \frac{\partial^2}{\partial \eta^2}\tilde{\psi} = \beta_{\tilde{\omega}}\hat{\Upsilon}_0[\tilde{\omega} + \tilde{f}]\,[He(\xi) - He(\xi - \tilde{l})]\delta(\eta + 1) \quad (69)$$

$$\beta_{\tilde{\omega}} = \frac{}{\tilde{\omega}^2 - (\tilde{f}^2 + \tilde{\lambda}^2)}$$

$$\eta = z/h \qquad \xi = \frac{x}{h}\frac{[\tilde{\omega}^2 - (\tilde{f}^2 + \tilde{\lambda}^2)]^{1/2}}{\tilde{N}}$$

In (69) we have made the hydrostatic approximation. The waves which satisfy (69) are of the form

$$\tilde{\psi}\cos(\tilde{\omega}\tau) = -\beta^{-}\Upsilon_0[\tilde{\omega} + \tilde{f}]$$

$$\cdot \sum_{n=1}^{\infty}\frac{4}{\tilde{l}k_n^2}\sin(k_n\xi)[\sin k_n\eta_+ + \sin k_n\eta_-$$

$$\cos(\tilde{\omega}\tau) \qquad k_n = \frac{\cdots}{\tilde{l}} \quad (70)$$

In the space of nondimensional coordinates, the waves propagate at an angle $\pi/4$. Figure 7 shows the structure of these waves at a given time in dimensional space.

Since a right combination is needed: a region in low latitude where the dissipation is negligible and where the wind stress is persistent and periodic, these waves are probably a rare event.

8. SUMMARY OF THE MAIN RESULTS

The characteristic time scale for the upwelling is $T = (f^2 + \lambda^2)^{-1/2}$ and the relevant Rossby deformation radius is $R = hN(f^2 + \lambda^2)^{-1/2}$. These scales clearly show that inertia and friction both equally contribute to T and R. At a distance from the coast larger than R the intensity of the upwelling rapidly decreases for a horizontally uniform wind stress. The horizontal scale of the upwelling R can be enhanced by nonuniform wind stress, with positive horizontal gradients. If the horizontal gradient of the wind stress is negative, the

horizontal scale of the upwelling is smaller than R. Under patchy wind stress forcing, the sea current response is patchy if the wind stress patches are larger than $2R$, otherwise the patches merge together. The maximum intensity of the upwelling occurs near the coast at a depth equal to the depth of the stress h, and deeper far from the coast in an infinite deep sea.

A stationary state or a periodic state is reached only after a number of characteristic times (several days if the motion is almost frictionless). In the presence of friction, a stationary state or a pure periodic state is reached when $t > 3\lambda^{-1}$. Periodicity in the forcing enhances the intensity, the characteristic time, and the horizontal scale of the upwelling.

A wave pattern can arise below 30° latitude under periodic forcing if the damping due to friction is small.

Appendix A: Definition of the Nondimensional Variables

We define the following nondimensional quantities:

$$T = \frac{1}{(f^2 + \lambda^2)^{1/2}} \qquad \tilde{f} = fT \qquad \tilde{N} = NT \qquad \tilde{\lambda} = \lambda T$$

$$= \frac{}{\partial \tau} \qquad p = s + \tilde{\lambda} \qquad \tilde{\omega} = \omega T$$

$$\eta = z/h \qquad \tau = tT^{-1}$$

$$\xi = \left(\frac{\tilde{f}^2 + p^2}{\tilde{N}^2 + p^2}\right)^{1/2} \frac{x}{h} \approx \frac{(\tilde{f}^2 + p^2)^{1/2}}{\tilde{N}} \frac{x}{h}$$

$$\left(\frac{\tilde{f}^2 + p^2}{\tilde{N}^2 + p^2}\right)^{1/2} \frac{y}{h} \approx \frac{(\tilde{f}^2 + p^2)^{1/2}}{\tilde{N}} \frac{y}{h}$$

$$\tilde{H} = H/h \qquad \tilde{h}_n = h_n/h$$

$$\tilde{l}_n = \left(\frac{\tilde{f}^2 + p^2}{\tilde{N}^2 + p^2}\right)^{1/2} \frac{l_n}{h} \approx \frac{(\tilde{f}^2 + p^2)^{1/2}}{\tilde{N}} \frac{\iota_n}{h}$$

where

$$\hat{f}(s) = L\{f(\tau)\} = \int_0^\infty f(\tau) \exp(-s\tau)\, d\tau$$

$$LL^{-1}\{f(\tau)\} = f(\tau)$$

$$\hat{\psi} = L\{\psi h^{-2} T\} \qquad \tilde{\psi} = \psi h^{-2} T$$

$$(\hat{u}, \hat{v}, \hat{w}) = L\{(u, v, w) h^{-1} T\} \qquad (\tilde{u}, \tilde{v}, \tilde{w}) = (u, v, w) h^{-1} T$$

$$\hat{b} = L\{b h^{-1} T^2\} \qquad \tilde{b} = b h^{-1} T^2$$

$$\hat{Q} = L\{Q h^{-2} T^3\} \qquad \tilde{Q} = Q h^{-2} T^3$$

$$\hat{\Upsilon} = L\{\Upsilon h^{-2} T\} \qquad \tilde{\Upsilon} = \Upsilon h^{-2} T$$

$$\hat{\Phi} = L\{\Phi h^{-2} T^2\} \qquad \tilde{\Phi} = \Phi h^{-2} T^2$$

$$\beta(p) = \frac{}{\tilde{f}^2 + p^2}$$

$$\beta'(p) = \left(\frac{1}{\tilde{N}^2 + p^2}\right)^{1/2} \left(\frac{1}{\tilde{f}^2 + p^2}\right)^{1/2} \approx \frac{}{\tilde{N}\,(\tilde{f}^2 + p^2)^{1/2}}$$

In (A1) the approximation is the hydrostatic approximation. T is the characteristic time scale and h is the depth of the mixed layer, i.e., the depth through which the mechanical forcing Υ and the thermal forcing Q are acting. L is the Laplace transform operator; the variables with the circumflexes are Laplace transformed. The variables with the tildes are nondimensional.

Appendix B: Green Functions for the Velocities

From the Green function of the stream function (equation (11)), we deduce through derivation the Green functions of the horizontal velocity for a finite deep sea,

$$g_u = \frac{\partial}{\partial \eta} g_\psi = \frac{1}{4\tilde{H}} \left\{ \frac{\sin(\pi/\tilde{H})\eta_{0-}}{\cosh(\pi/\tilde{H})\xi_{0-} - \cos(\pi/\tilde{H})\eta_{0-}} + \frac{\sin(\pi/\tilde{H})\eta_{0+}}{\cosh(\pi/\tilde{H})\xi_{0+} - \cos(\pi/\tilde{H})\eta_{0+}} \right\}$$

$$\frac{}{4\tilde{H}} \left\{ \frac{\sin(\pi/\tilde{H})\eta_{0+}}{\cosh(\pi/\tilde{H})\xi_{0-} - \cos(\pi/\tilde{H})\eta_{0+}} + \frac{\sin(\pi/\tilde{H})\eta_{0-}}{\cosh(\pi/\tilde{H})\xi_{0+} - \cos(\pi/\tilde{H})\eta_{0-}} \right\} \tag{B1}$$

and the vertical velocity,

$$g_w = -\frac{\partial}{\partial \xi} g_\psi = \frac{}{4\tilde{H}} \left\{ \frac{\sinh(\pi/\tilde{H})\xi_{0-}}{\cosh(\pi/\tilde{H})\xi_{0-} - \cos(\pi/\tilde{H})\eta_{0-}} + \frac{\sinh(\pi/\tilde{H})\xi_{0+}}{\cosh(\pi/\tilde{H})\xi_{0+} - \cos(\pi/\tilde{H})\eta_{0+}} \right\}$$

$$\frac{1}{4\tilde{H}} \left\{ \frac{\sinh(\pi/\tilde{H})\xi_{0-}}{\cosh(\pi/\tilde{H})\xi_{0-} - \cos(\pi/\tilde{H})\eta_{0+}} + \frac{\sinh(\pi/\tilde{H})\xi_{0+}}{\cosh(\pi/\tilde{H})\xi_{0+} - \cos(\pi/\tilde{H})\eta_{0-}} \right\} \tag{B2}$$

From the Green function (equation (12)) we deduce through derivation the Green functions of the horizontal velocity for an infinitely deep sea,

$$g_u = \frac{\partial}{\partial \eta} g_\psi = \frac{1}{2\pi} \left\{ \frac{\eta_{0-}}{\xi_{0-}^2 + \eta_{0-}^2} + \frac{\eta_{0+}}{\xi_{0+}^2 + \eta_{0+}^2} \right\}$$

$$- \frac{1}{2\pi} \left\{ \frac{\eta_{0+}}{\xi_{0-}^2 + \eta_{0+}^2} + \frac{\eta_{0-}}{\xi_{0+}^2 + \eta_{0-}^2} \right\} \tag{B3}$$

and for the vertical velocity,

$$g_w = -\frac{\partial}{\partial \xi} g_\psi = -\frac{1}{2\pi} \left\{ \frac{\xi_{0-}}{\xi_{0-}^2 + \eta_{0-}^2} + \frac{\xi_{0+}}{\xi_{0+}^2 + \eta_{0+}^2} \right\}$$

$$+ \frac{1}{2\pi} \left\{ \frac{\xi_{0-}}{\xi_{0-}^2 + \eta_{0+}^2} + \frac{\xi_{0+}}{\xi_{0+}^2 + \eta_{0-}^2} \right\} \tag{B4}$$

$$\xi_{0+} = (\xi + \xi') \qquad \xi_{0-} = (\xi - \xi')$$

$$\eta_{0+} = (\eta + \eta') \qquad \eta_{0-} = (\eta - \eta')$$

APPENDIX C: THE $\hat{S}^n$ FUNCTIONS

From (34), using (35), we can compute the $\hat{S}^n(\xi, \eta)$ functions in (51). For an infinite deep sea,

$$\hat{S}^n_{\psi Y}(\xi, \eta) = \frac{}{2\pi}\{\xi_- \ln[\xi_-^2 + \eta_+^2]^{1/2} + \xi_+ \ln[\xi_+^2 + \eta_+^2]^{1/2} - \xi_- \ln[\xi_-^2 + \eta_-^2]^{1/2} - \xi_+ \ln[\xi_+^2 + \eta_-^2]^{1/2}\} + \frac{1}{2\pi}\left\{\eta_+ \left| \frac{\xi_-}{\eta_+} + \tan^{-1}\frac{\xi_+}{\eta_+} \right. - \eta_- \left[\tan^{-1}\frac{\xi_-}{\eta_-} + \tan^{-1}\frac{\xi_+}{\eta_-}\right]\right\} \quad \text{(C1a)}$$

$$\hat{S}^n_{uY}(\xi, \eta) = \frac{}{2\pi}\left\{ \frac{\xi_+}{\eta_+} + \tan \frac{\xi_-}{\eta_+} - \tan^{-1}\frac{\xi_-}{\eta_-} - \tan^{-1}\frac{\xi_+}{\eta_-}\right\} \quad \text{(C1b)}$$

$$\hat{S}^n_{wY}(\xi, \eta) = -\frac{}{2\pi}\ln\left[\frac{\xi_-^2 + \eta_+^2}{\xi_+^2 + \eta_-^2}\frac{\xi_+^2 + \eta_+^2}{\xi_-^2 + \eta_-^2}\right]^{1/2} \quad \text{(C1c)}$$

$$\hat{S}^n_{vY}(\xi, \eta) = He(\xi_-)He(\eta_+) \quad \text{(C1d)}$$

For a sea of finite depth,

$$\hat{S}^n_{uY}(\xi, \eta) = \frac{1}{2\pi}\left\{\tan^{-1}\frac{\tanh(\pi/2\tilde{H})\xi}{\tan(\pi/2\tilde{H})\eta_+} + \tan \frac{\tanh(\pi/2\tilde{H})\xi_-}{\tan(\pi/2\tilde{H})\eta_+} - \tan^{-1}\frac{\tanh(\pi/2\tilde{H})\xi_-}{\tan(\pi/2\tilde{H})\eta_-} - \tan \frac{\tanh(\pi/2\tilde{H})\xi_+}{\tan(\pi/2\tilde{H})\eta_-}\right\}$$

$$\hat{S}^n_{wY}(\xi, \eta) = -\frac{}{2\pi}\left\{\ln\left[\frac{\cosh(\pi/\tilde{H})\xi_- - \cos(\pi/\tilde{H})\eta_+}{\cosh(\pi/\tilde{H})\xi_+ - \cos(\pi/\tilde{H})\eta_-}\frac{\cosh(\pi/\tilde{H})\xi_+ - \cos(\pi/\tilde{H})\eta_+}{\cosh(\pi/\tilde{H})\xi_- - \cos(\pi/\tilde{H})\eta_-}\right]^{1/2}\right\}$$

$$\xi_+ = (\xi + \tilde{l}_n) \qquad \xi_- = (\xi - \tilde{l}_n)$$

$$\eta_+ = (\eta + \tilde{h}_n) \qquad \eta_- = (\eta - \tilde{h}_n)$$

Acknowledgments. We wish to acknowledge the contribution of the reviewers in helping to clarify some of the physical aspects of the upwelling described in this paper. We acknowledge the support of the Cooperative Institute for Research in the Atmosphere (CIRA), of the National Science Foundation (NSF), under contract ATM-8616662, and the Office of Naval Research, under contract N000H-88-K-0029. G.A.D. acknowledges the support of the Italian Sistema Lagunare Vereziano.

REFERENCES

Allen, J. S., Upwelling and coastal jets in a continuously stratified ocean, *J. Phys. Oceanogr.*, *3*, 245–257, 1973.

ALPEX Group, Scientific results of the alpine experiment (ALPEX), *WMO/TD Rep. 108*, World Meteorol. Organ., Geneva, 1986.

Carton, J. S., and S. G. H. Philander, Coastal upwelling viewed as a stochastic phenomenon, *J. Phys. Oceanogr.*, *14*, 1499–1509, 1984.

Clancy, R. M., J. D. Thompson, H. E. Hulburt, and J. D. Lee, A model of mesoscale air-sea interaction in a sea-breeze coastal upwelling regime, *Mon. Weather Rev.*, *107*, 1476–1505, 1979.

Crepon, M., C. Richez, and M. Chartier, Effects of coastline geometry on upwelling, *J. Phys. Oceanogr.*, *14*, 1365–1382, 1984.

Dalu, G. A., and R. Purini, Un modello numerico della dinamica delle acque costiere accoppiato con un modello di circolazione di brezza, *Riv. Ing. Sanit.*, *5*, 235–238, 1980.

Dalu, G. A., and R. Purini, A numerical study of the marine surface layer in a sea breeze regime, *Ocean Manage.*, *6*, 111–116, 1981.

Dalu, G. A., M. Baldi, and C. Lavalle, Upwelling induced by periodic wind stress, *Nuovo Cimento Soc. Ital. Fis.*, *11C*, 739–746, 1989.

Defant, A., *Physical Oceanography*, pp. 41–42, Pergamon, New York, 1961.

Dewey, R. K., and W. R. Crawford, Bottom stress estimates from vertical dissipation rate profiles on the continental shelf, *J. Phys. Oceanogr.*, *18*, 1167–1177, 1988.

Fodor, G., *Laplace Transform in Engineering*, Hungarian Academy of Science, Budapest, 1965.

Geernaert, G., Drag coefficient modelling for the near coastal zone, *Dyn. Atmos. Oceans*, *11*, 307–322, 1988.

Huss, A., and Y. Feliks, A mesometeorological model of the sea and land breeze involving sea-atmosphere interaction, *Contrib. Atmos. Phys.*, *54*, 238–257, 1981.

Kundu, P. K., Generation of coastal inertial oscillations by time-varying wind, *J. Phys. Oceanogr.*, *14*, 1901–1913, 1984.

Middleton, J. H., and R. E. Thompson, Steady wind driven coastal circulation on a β-plane, *J. Phys. Oceanogr.*, *15*, 1809–1817, 1985.

Mizzi, A. P., and R. A. Pielke, A numerical study of the atmospheric circulation observed during a coastal upwelling event on 23 August 1972, I, Sensitivity studies, *Mon. Weather Rev.*, *112*, 76–90, 1984.

Mofjeld, H. O., Depth dependence of the bottom stress and quadratic drag coefficient for barotropic pressure-driven currents, *J. Phys. Oceanogr.*, *18*, 1658–1669, 1988.

Niino, H., The linear theory of land and sea breeze circulation, *J. Meteorol. Soc. Jpn.*, *65*(6), 901–920, 1987.

Pedlosky, J., *Geophysical Fluid Dynamics*, 624 pp., Springer-Verlag, New York, 1979.

Richards, F. A. (Ed.), *Coastal Upwelling*, *Coastal Estuarine Sci.*, vol. 1, 529 pp., AGU, Washington, D. C., 1981.

Roll, H. U., *Physics of the Marine Atmosphere*, Academic, San Diego, Calif., 1965.

Rotunno, R., On the linear theory of land and sea breeze, *J. Atmos. Sci.*, *40*, 1999–2009, 1983.

Salat, J., J. Font, J. Tintoré, and D. P. Wang, Inertial oscillations in a shelf/slope region of the northwestern Mediterranean, paper presented at European Geophysical Society Conference, Eur. Geophys. Soc., Barcelona, Spain, 1989.

Winant, C. D., Coastal circulation and wind induced currents, *Annu. Rev. Fluid Mech.*, *12*, 271–301, 1980.

Winant, C. D., C. E. Dorman, C. A. Friehe, and R. C. Beardsley, The marine layer off the northern California: An example of supercritical channel flow, *J. Atmos. Sci.*, *45*, 3588–3605, 1988.

G. A. Dalu and R. A. Pielke, Colorado State University, CIRA, Foothill Campus, Fort Collins, CO 80523.

(Received November 7, 1988;
accepted May 2, 1989.)